Electronic Supplementary Material (ESI) for Sustainable Energy & Fuels.

Electronic Supplementary Information

Co-catalyst Design to Control Charge Transfer and Product Composition for Photocatalytic H_2 Production and Biomass Reforming

Van-Can Nguyen,[a] Meyta Sanoe,[a] Novy Pralisa Putri,[a] Yuh-Lang Lee,[a,b] and Hsisheng Teng[a,b,*]

[a]Department of Chemical Engineering, National Cheng Kung University, Tainan 70101, Taiwan

[b]Hierarchical Green-Energy Materials (Hi-GEM) Research Center, National Cheng Kung University, Tainan 70101, Taiwan

*To whom correspondence should be addressed. (E-mail): hteng@mail.ncku.edu.tw

(Fax): 886-6-2344496

Supporting Data and Results

1. TEM and HR-TEM images of SNGODs

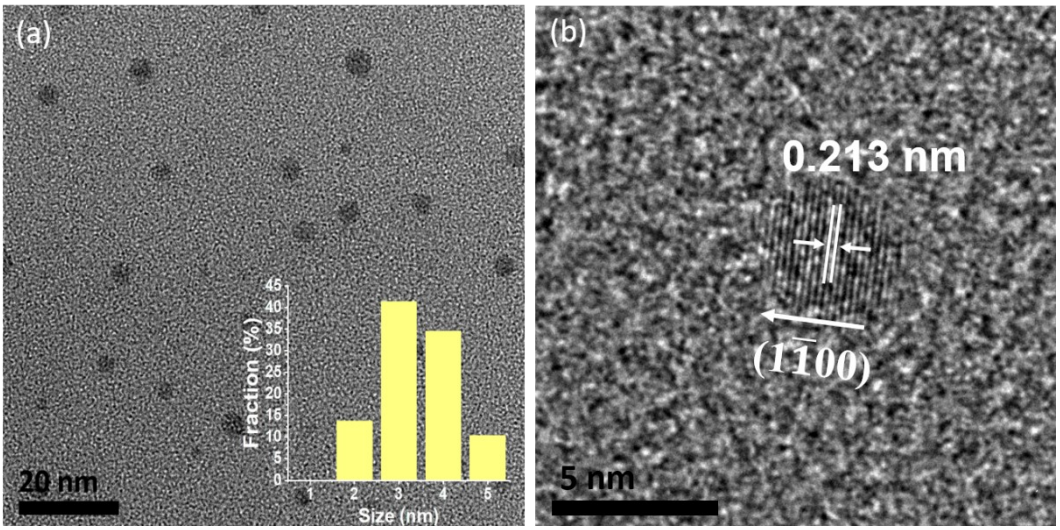

Fig. S1 Morphology and crystal structure of the SNGODs. (a) TEM image of the SNGOD particles and the inset histogram of the particle size distribution. (b) High-resolution TEM image of an SNGOD particle.

2. TEM and HR-TEM images of Pt-SNGODs

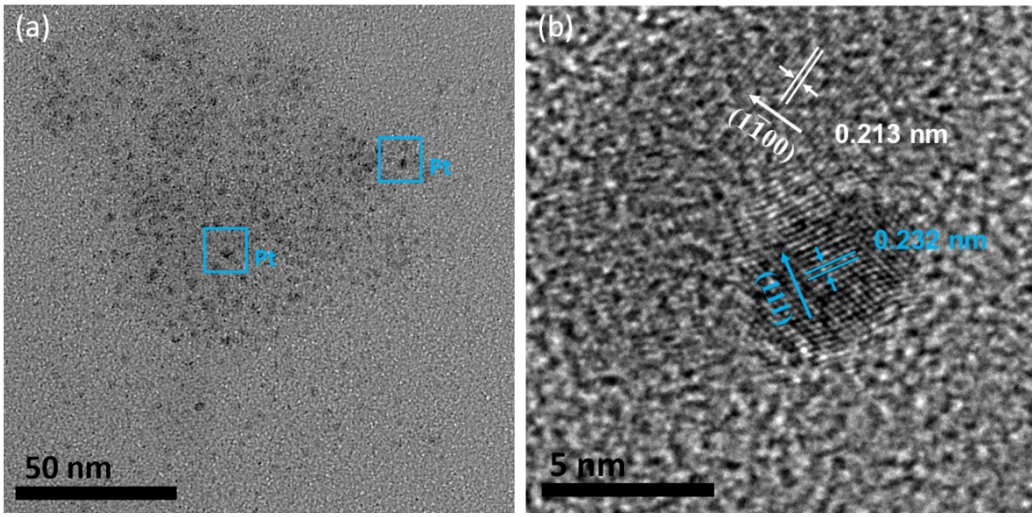

Fig. S2 TEM and HR-TEM images of Pt-SNGODs on GO sheets. (a) TEM image of the SNGOD and Pt particles. (b) High-resolution TEM image of the SNGOD and Pt particles.

3. TEM and HR-TEM images of Ag-SNGODs

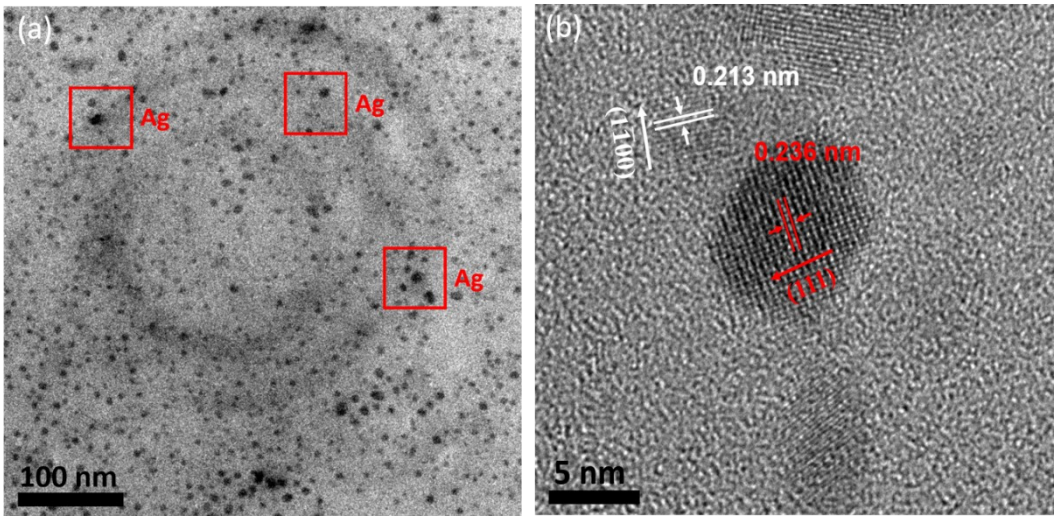

Fig. S3 TEM and HR-TEM images of Ag-SNGODs on GO sheets. (a) TEM image of the SNGOD and Ag particles. (b) High-resolution TEM image of the SNGOD and Ag particles.

4. XPS spectra of SNGODs

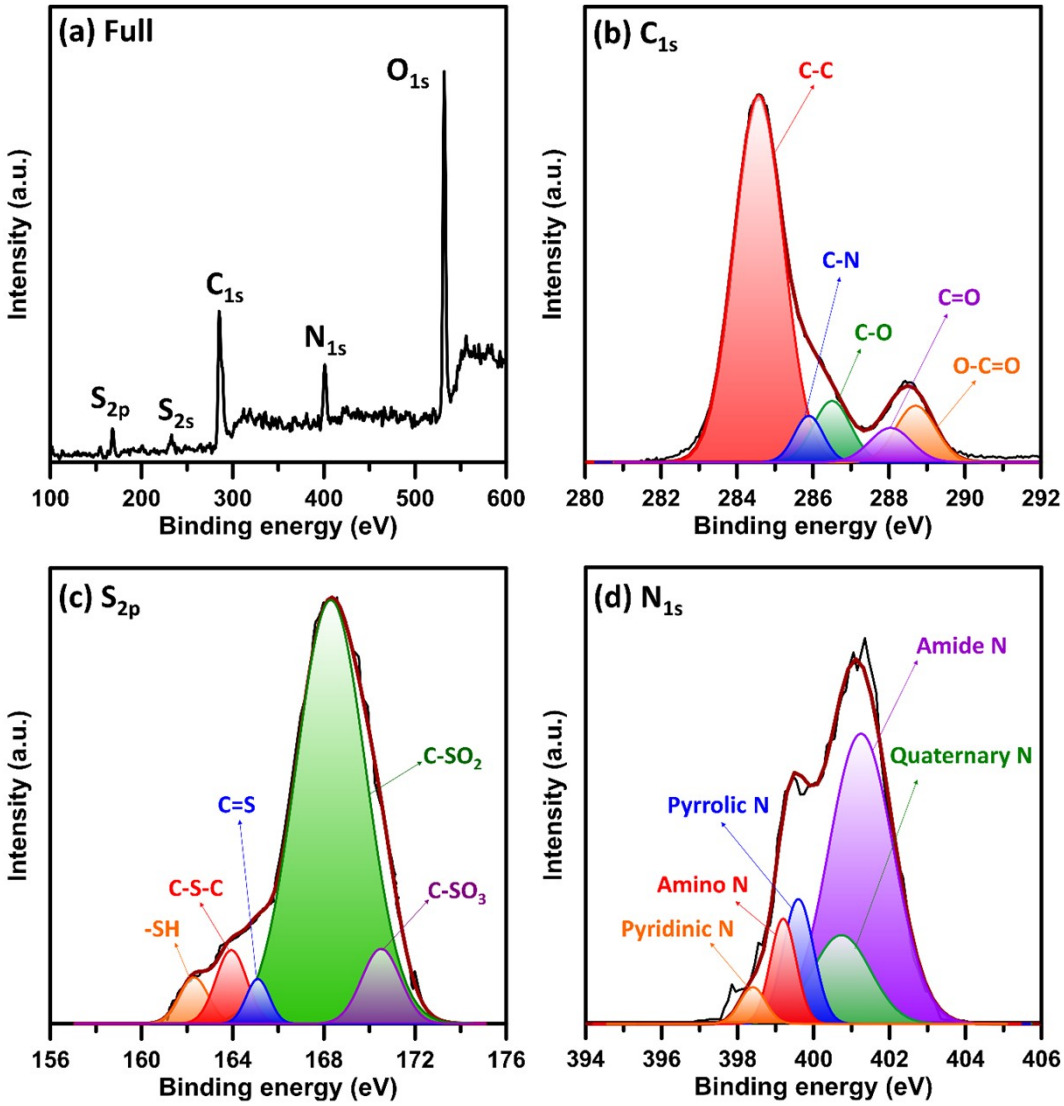

Fig. S4 XPS spectra of SNGODs. (a) Full-range spectrum. (b) C_{1s} spectrum. (c) S_{2p} spectrum. (d) N_{1s} spectrum. The C_{1s}, S_{2p}, and N_{1s} spectra were deconvoluted into their constituent peaks.

Table S1 Atomic ratios of O_{1s}/C_{1s}, N_{1s}/C_{1s}, and S_{2p}/C_{1s} determined from the full-range XPS spectrum (Fig. S4a) and its deconvoluted functionalities (Figs. S4b-S4d) for the SNGOD photocatalyst

Atomic ratio	Carbon bonding composition (%)				
O_{1s}/C_{1s}	C–C	C–N	C–O	C=O	O–C=O
40%	71	5.3	9.0	5.6	8.9
Atomic ratio	Nitrogen functionality composition (% of C_{1s})				
N_{1s}/C_{1s}	pyridine	amino	pyrrolic	quaternary	amide
11%	0.32	0.92	1.3	1.7	6.3
Atomic ratio	Sulfur functionality composition (% of C_{1s})				
S_{2p}/C_{1s}	–SH	C–S–C	C=S	$C–SO_2$	$C–SO_3$
7%	0.26	0.44	0.20	5.7	0.56

5. XPS spectra of Pt-SNGODs and Ag-SNGODs

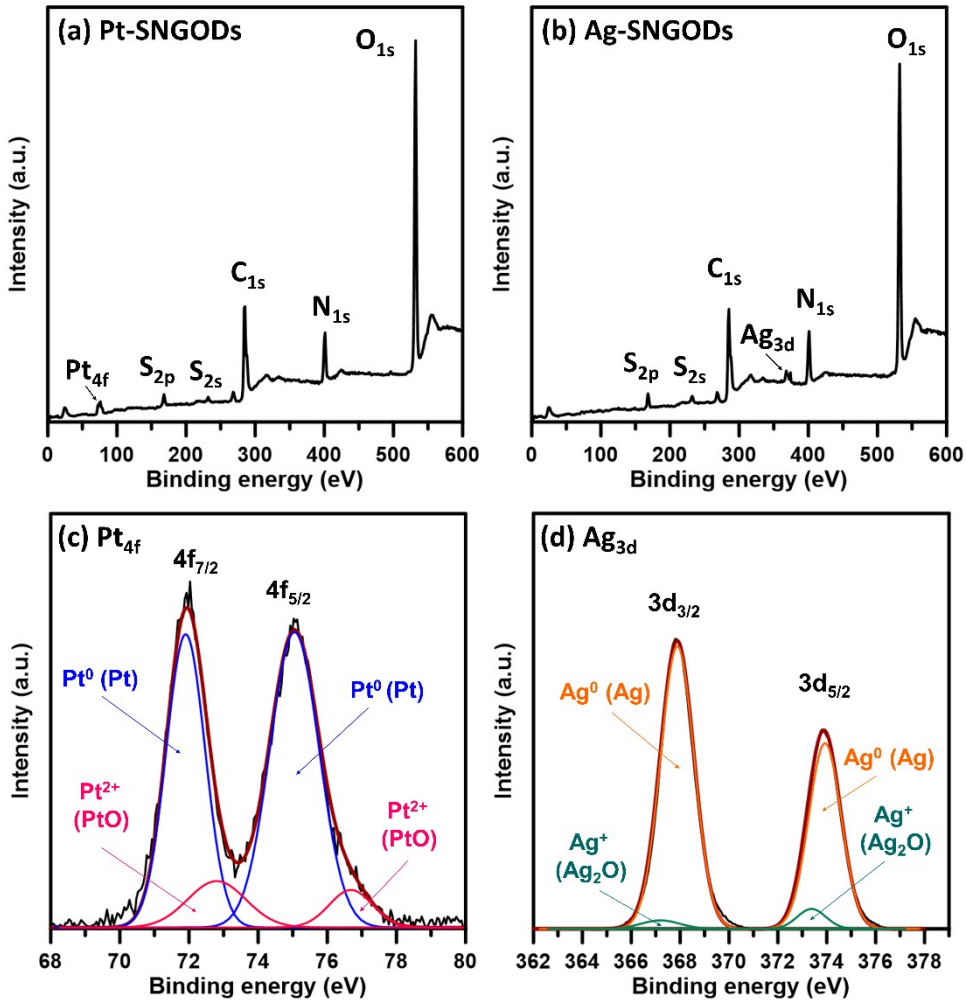

Fig. S5 XPS spectra of Pt-SNGODs and Ag-SNGODs. Full-range of (a) Pt-SNGODs and (b) Ag-SNGODs; high-resolution of (c) Pt_{4f} and (d) Ag_{3d}.

6. Absorption spectrum of xylose solution

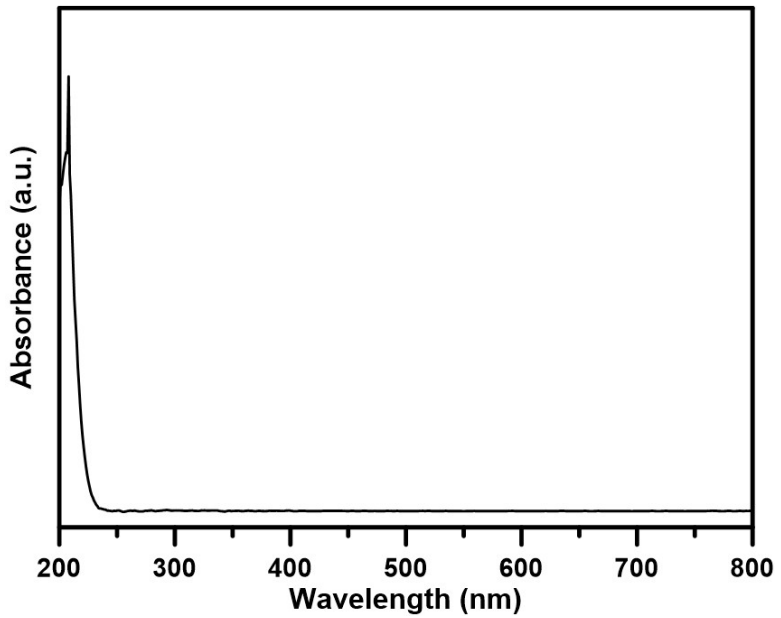

Fig. S6 Absorption spectrum of an aqueous xylose solution (10 g L^{-1}).

7. PL spectra of SNGODs with co-catalyst deposition and xylose presence

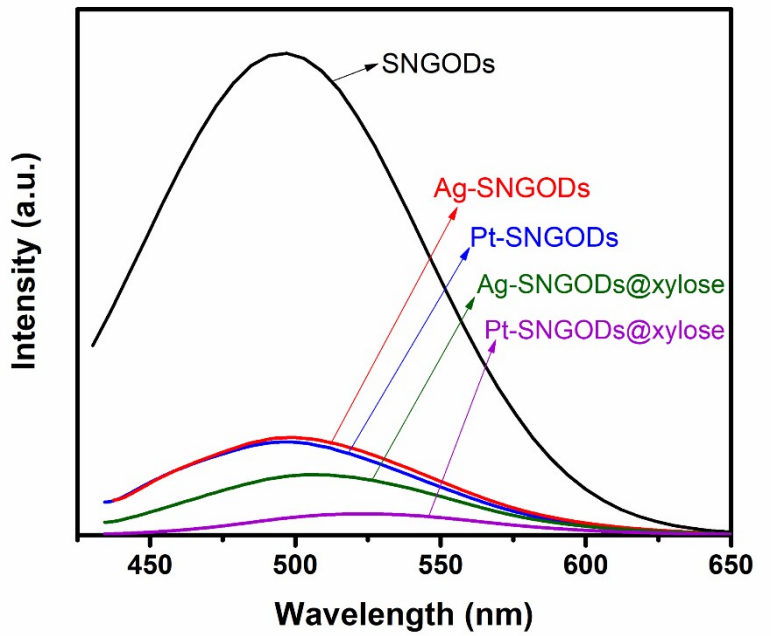

Fig. S7 Photoluminescence spectra of SNGODs, Pt-SNGODs, Ag-SNGODs, Pt-SNGODs@xylose, and Ag-SNGODs@xylose, which were excited at 405 nm.

8. TRPL decay of SNGODs with co-catalyst deposition and xylose presence

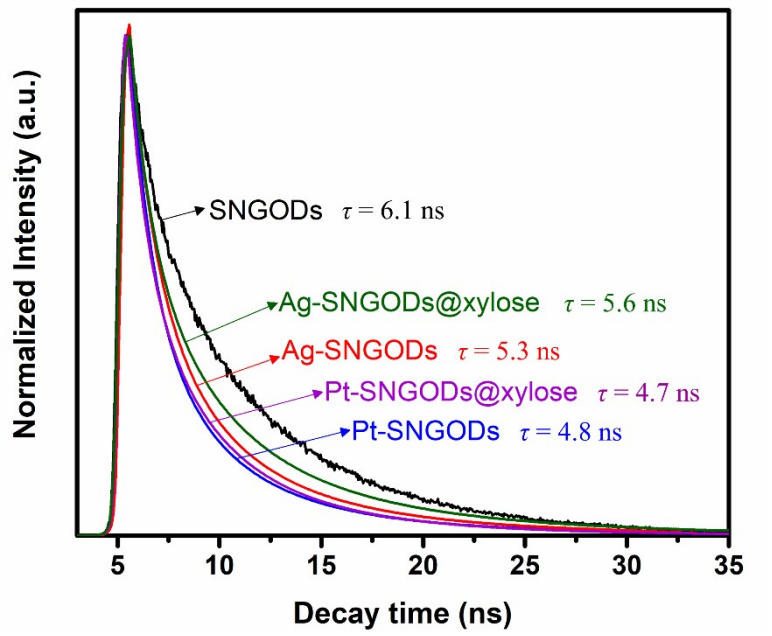

Fig. S8 Time-resolved PL decay curves of the SNGODs, Pt-SNGODs, Ag-SNGODs, Pt-SNGODs@xylose, and Ag-SNGODs@xylose, which were excited at 405 nm.

Table S2 The fitting parameters of the PL decay curves (Fig. S8), excited using a 405-nm laser, simulated under an exponential intensity function of $R(t) = Be^{-t/\tau}$, where R is the radiative recombination intensity, t is the elapsed time after excitation, B is a constant, and τ is emission lifetime.

	τ (ns)	B
SNGODs	17.4×10^{-1}	2.1×10^{1}
Pt-SNGODs	19.4×10^{-1}	3.6×10^{1}
Ag-SNGODs	15.5×10^{-1}	2.7×10^{1}
Pt-SNGODs@xylose	9.9×10^{-1}	2.8×10^{1}
Ag-SNGODs@xylose	9.3×10^{-1}	3.3×10^{1}

9. UPS spectra of SNGODs, Pt-SNGODs, and Ag-SNGODs

We identified the VBM level of the catalysts deposited on silicon substrate by using UPS equipped with He I light irradiation. The following equation was used for UPS analysis:

$$E_B + E_k + \varphi = 21.2$$

where E_B is the binding energy measured from the Fermi level (E_F), E_k is the kinetic energy of electrons, φ is the work function of the catalysts, and 21.2 eV is the energy of the He I light.

The VBM and E_F can be calculated using the following equations:

$$\text{VBM} = 21.2 - (E_{B2} - E_{B1})$$

$$E_F = 21.2 - E_{B2}$$

where E_{B2} is the secondary cutoff binding energy in the UPS spectra, in which the E_k of the excited electrons is equal to 0, and E_{B1} represents the difference between the E_F and VBM levels. **Fig. S9** shows the UPS spectra of the catalysts. The E_{B1} can be determined using the intercepts of the extrapolated straight lines on the abscissa at low binding energy. The E_{B2} can be estimated using the secondary cutoff values ($E_k = 0$ eV) in the UPS spectra, obtained from the intercepts of the extrapolated straight lines on the abscissa at high binding energy. The UPS widths are the difference between E_{B2} and E_{B1}. As presented in the above two equations, we determined the VBM level relative to the vacuum by subtracting the width of the UPS spectra ($E_{B2} - E_{B1}$) from the excitation energy (21.2 eV).

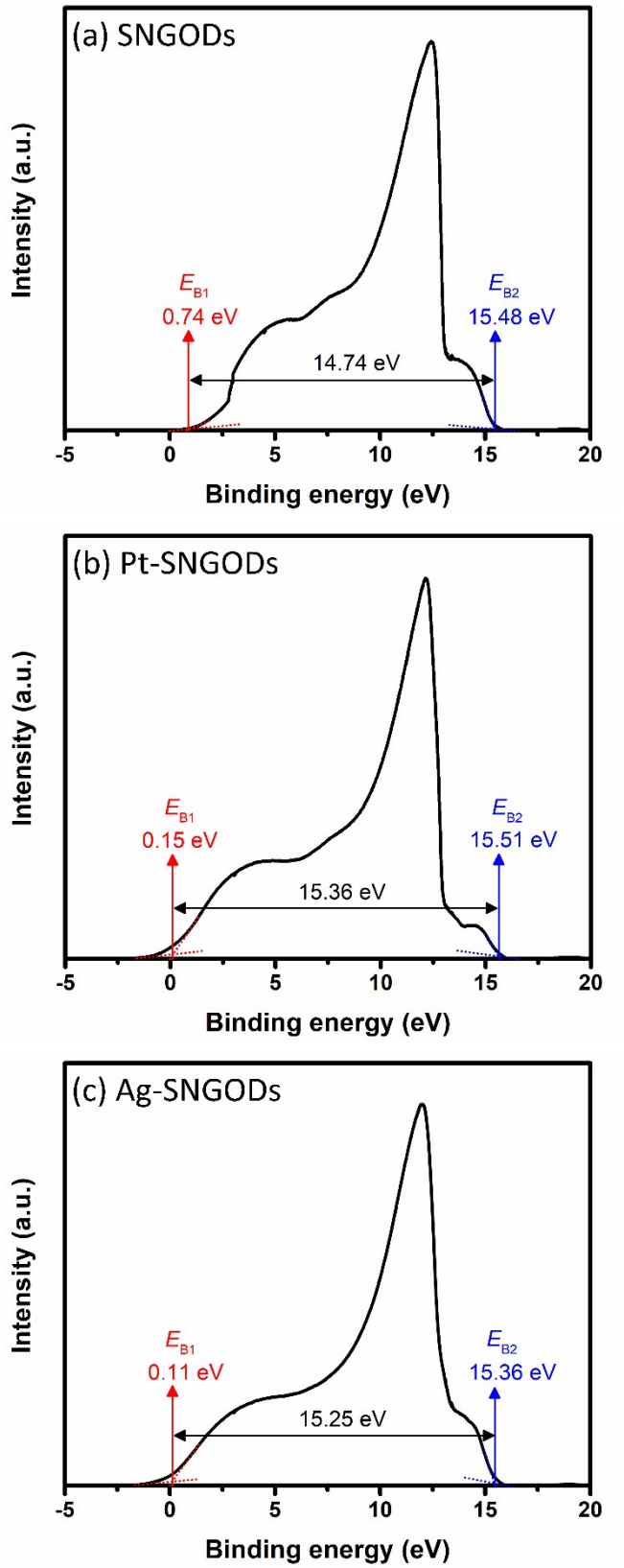

Fig. S9 UPS spectra of (a) SNGODs, (b) Pt-SNGODs, and (c) Ag-SNGODs. The UPS widths (black lines) can be determined by these two intercept binding energies, and the VBM can be calculated by subtracting these widths from the excitation energy (21.2 eV).

10. Tauc plots of SNGODs, Pt-SNGODs, and Ag-SNGODs

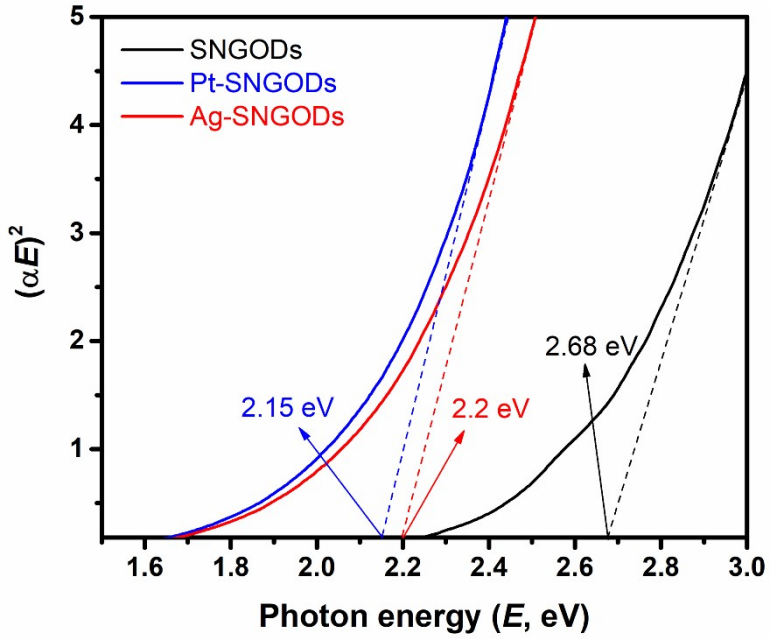

Fig. S10 Tauc plots obtained from the absorption spectra of the SNGODs, Pt-SNGODs, and Ag-SNGODs.

11. GC-TCD analysis of gas products from xylose photoreforming

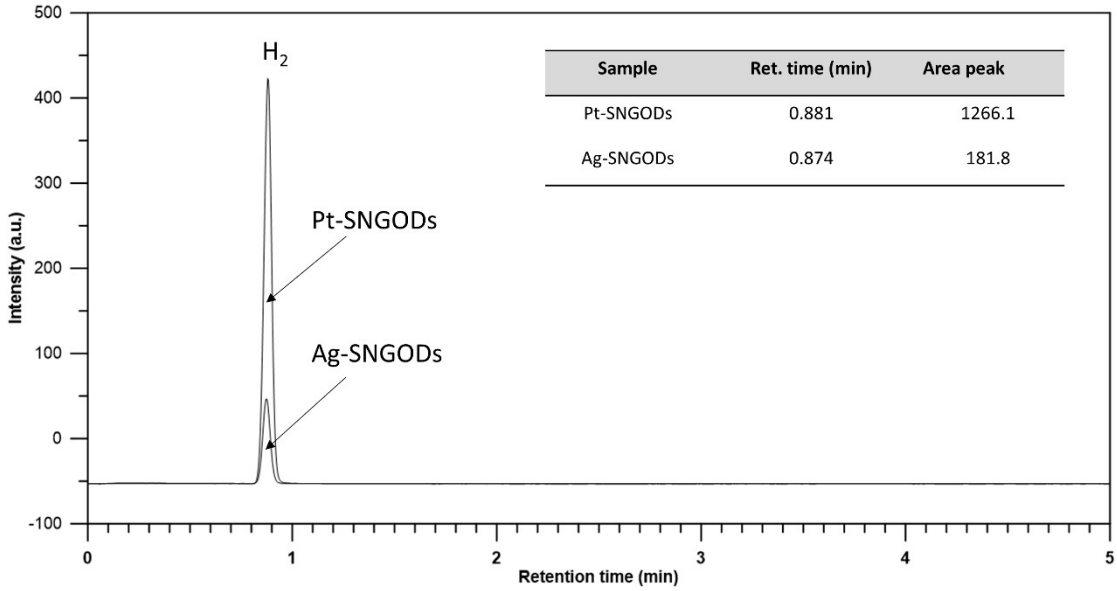

Sample	Ret. time (min)	Area peak
Pt-SNGODs	0.881	1266.1
Ag-SNGODs	0.874	181.8

Fig. S11 Gas product analysis using GC-TCD during the last 12 h of xylose photoreforming over Pt-SNGODs and Ag-SNGODs. The photo-reforming reaction was performed for 72 h with evacuating interventions every 12 h of irradiation.

12. Reaction of the Pt-deposited SNGOD catalysts w/ and w/o GO

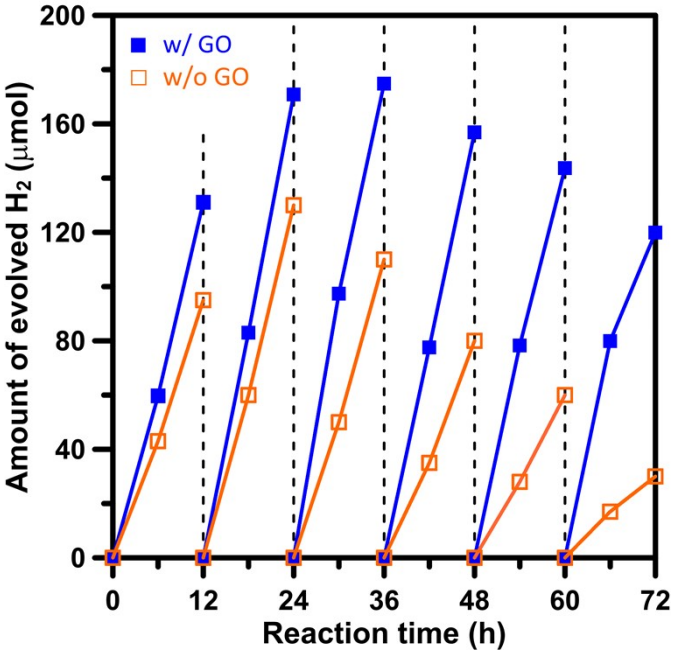

Fig. S12 The influence of GO-incorporation on the H_2 evolution from the xylose reforming over Pt-SNGODs (w/ GO or w/o GO). The reaction of the xylose solution (pH = 9) was performed in a gas-enclosed system, which was irradiated with 1 sun simulated light (AM 1.5G at 100 mW cm^{-2}) at 25 °C.

13. Reported photocatalytic H_2 production from mono-sugar solutions

Table S3. H_2 production from photocatalytic reforming of aqueous mono-sugar solutions.

Photocatalyst	**Substrate**	**Light source**	**H_2 evolution rate**	**Stability**	**AQY (%)**	**Ref.**
Pt-Sn/TiO_2 (50 mg) Pt-TiO_2 (50 mg)	Glucose (100 mg)	UV	330 (μmol $g^{-1}h^{-1}$) 60 (μmol $g^{-1}h^{-1}$)		0.06 (365 nm) 0.01 (365 nm)	1
$Zn_{0.6}Cd_{0.4}S$ (10 mg)	Glucose (240 mg)	Xe lamp	690 (μmol $g^{-1}h^{-1}$)	20 h	0.18 (420 nm)	2
Pt-ZnS-g-C_3N_4 (50 mg)	Glucose (50 ppm)	Xe lamp	210 (μmolg^{-1})		_	3
Pt-UCN-$NA_{0.5}$ (20 mg)	Glucose (100 mg)	LED	31 (μmolh^{-1})	8 h	_	4
Au-TiO_2 (5 mg)	Glucose (50 mg)	Xe lamp	10.9 (mmol $g^{-1}h^{-1}$)	8 h	_	5
Ru-doped $LaFeO_3$ (0.12 mg)	Glucose (80 mg)	UV	554 (μmol $g^{-1}h^{-1}$)	4 h	_	6
Pt-F-TiO_2 (0.12 g)	Glucose (160 mg)	UV-LED	590 (μmol $g^{-1}h^{-1}$)	3 h	_	7
Pt-g-C_3N_4 (5 mg)	Glucose (0.1 M)	AM 1.5	1370 (μmol $g^{-1}h^{-1}$)		_	8
Polymeric CN 30 mg	Xylose (200 mg)	Xe lamp	122 (μmol h^{-1})	4 h	7.87 (420 nm)	9
Pt-SNGODs (0.2 g) Ag-SNGODs (0.2 g)	Xylose (1 g)	AM 1.5	15 (μmol h^{-1}) 2.3 (μmol h^{-1})	72 h	6.8 (420 nm) 2.8 (420 nm)	This work

14. LC-MS analysis of the solutions from xylose reforming by Pt-SNGODs

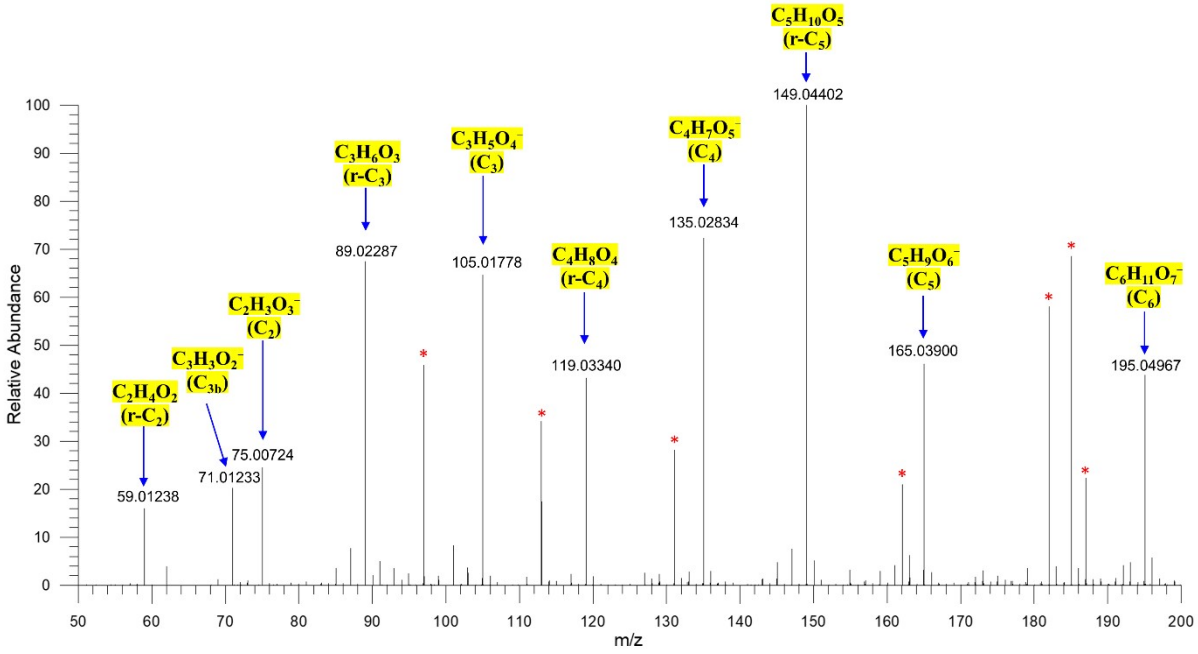

Fig. S13 LC-MS analysis shows the major deprotonated compounds obtained upon 72 h of photoreforming of xylose solutions by Pt-SNGODs. (*) unknown impurities that are irrelevant to this study.

Chemical Formula $[M-H]^-$	m/z	Δppm	RDB	Charge, z
$C_6H_{11}O_7^-$ (C_6)	195.04967	-1.329	1.5	1
$C_5H_9O_6^-$ (C_5)	165.03900	-2.208	1.5	1
$C_5H_{10}O_5$ (r-C_5)	149.04402	-2.884	1.5	1
$C_4H_7O_5^-$ (C_4)	135.02834	-3.405	1.5	1
$C_4H_8O_4$ (r-C_4)	119.03340	-4.076	1.5	1
$C_3H_5O_4^-$ (C_3)	105.01778	-4.334	1.5	1
$C_3H_6O_3$ (r-C_3)	89.02287	-5.061	1.5	1
$C_2H_3O_3^-$ (C_2)	75.00724	-1.739	1.5	1
$C_3H_3O_2^-$ (C_{3b})	71.01233	-1.997	2.5	1
$C_2H_4O_2$ (r-C_2)	59.01238	-1.370	1.5	1

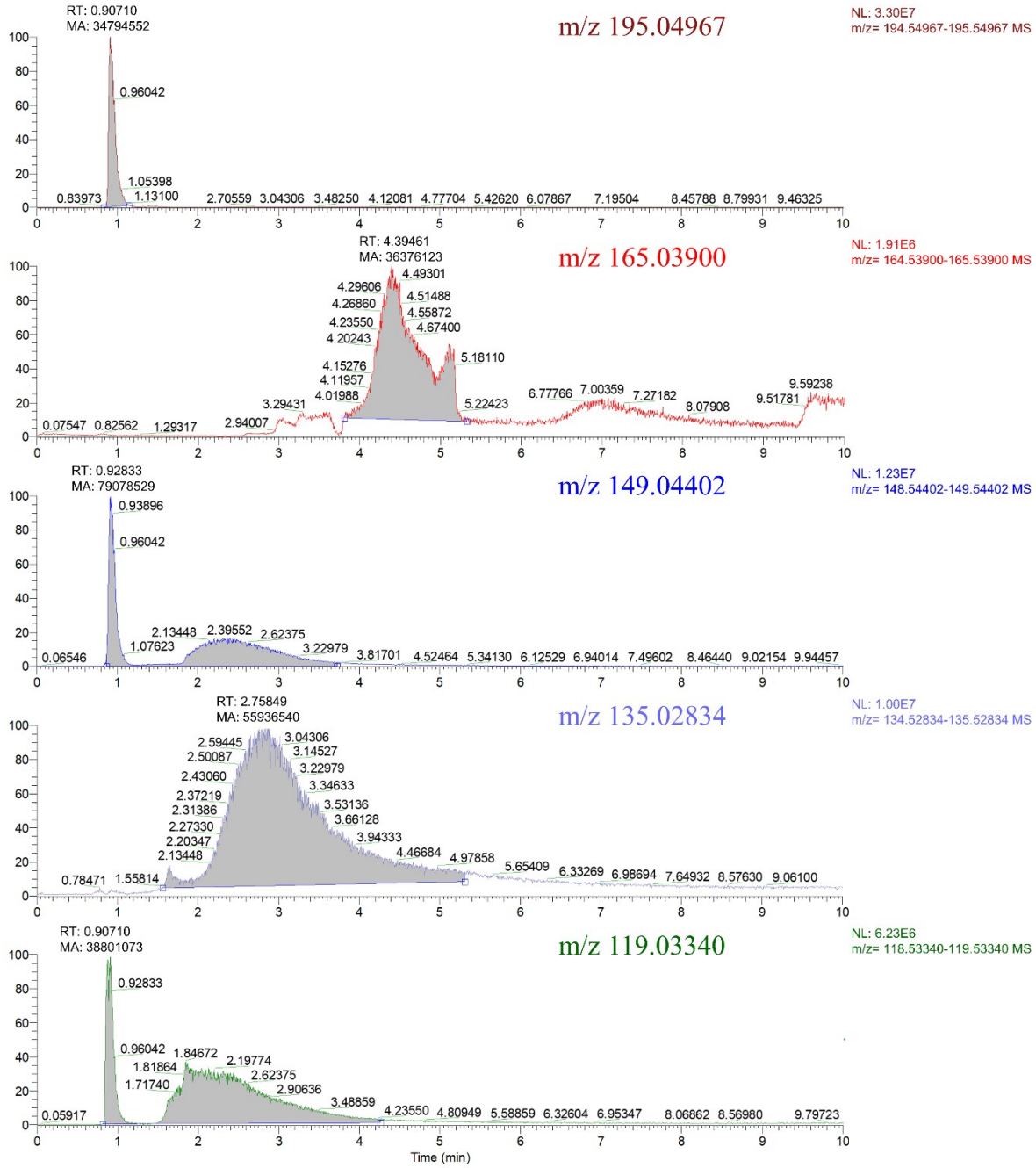

Fig. S14 Chromatograms for extracted-ions from LC-MS analysis in the solution of xylose photoreforming containing Pt-SNGODs.

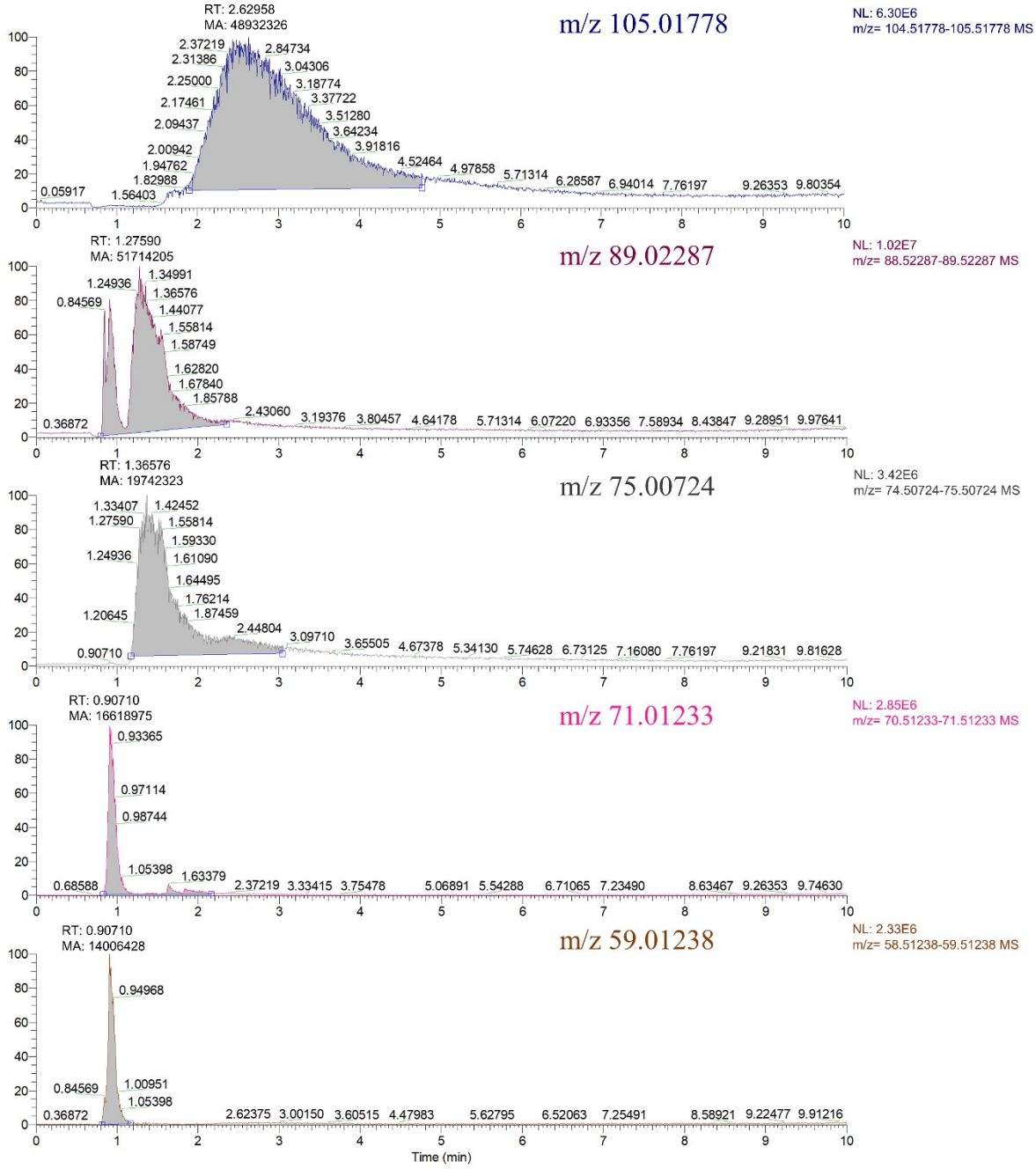

Fig. S15 (Cont'd) Chromatograms for extracted-ions from LC-MS analysis in the solution of xylose photoreforming containing Pt-SNGODs.

Chemical Formula	Retention time RT (min)	Base peak (m/z)	Measured Area MA
$C_6H_{11}O_7^-$ (C_6)	0.90710	195.04967	34794552
$C_5H_9O_6^-$ (C_5)	4.39461	165.03900	36376123
$C_5H_{10}O_5$ (r-C_5)	0.92833	149.04402	79078529
$C_4H_7O_5^-$ (C_4)	2.75849	135.02834	55936540
$C_4H_8O_4$ (r-C_4)	0.90710	119.03340	38801073
$C_3H_5O_4^-$ (C_3)	2.62958	105.01778	48932326

$C_3H_6O_3$ (r-C_3)	1.27590	89.02287	51714205
$C_2H_3O_3^-$ (C_2)	1.36576	75.00724	19742323
$C_3H_3O_2^-$ (C_{3b})	0.90710	71.01233	16618975
$C_2H_4O_2$ (r-C_2)	0.90710	59.01238	14006428

15. LC-MS analysis of the solutions from xylose reforming by Ag-SNGODs

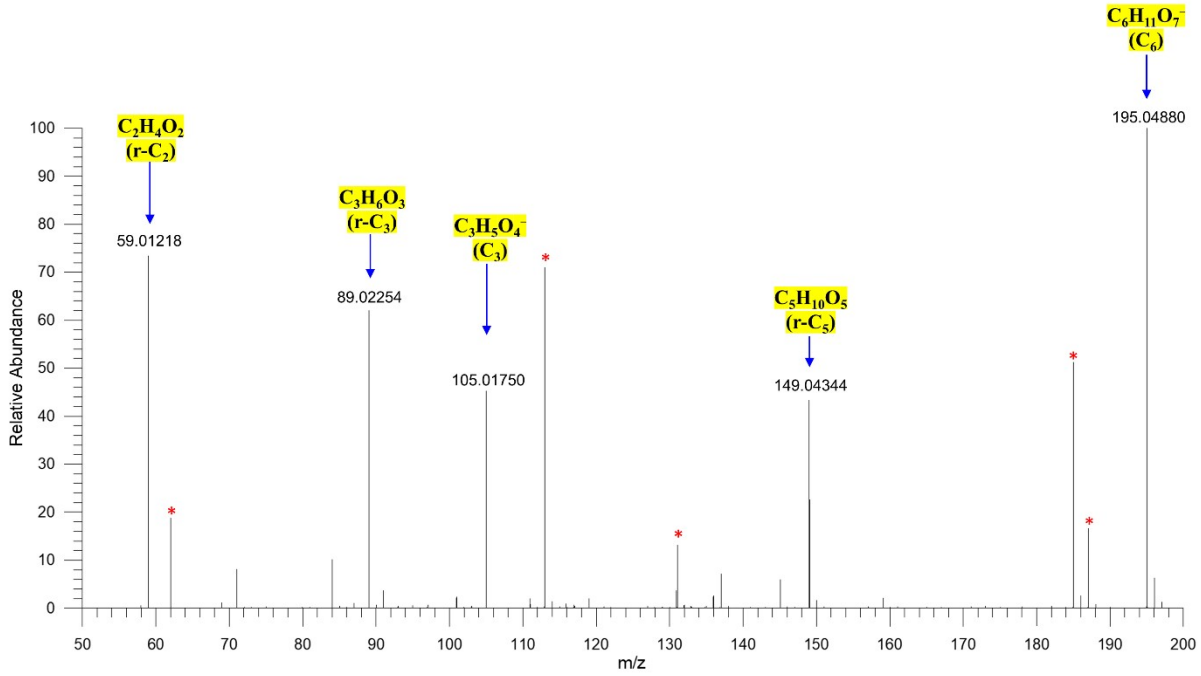

Fig. S16 LC-MS analysis shows the major deprotonated compounds obtained upon 72 h of photoreforming of xylose solutions by Ag-SNGODs. (*) unknown impurities that are irrelevant to this study.

Chemical Formula $[M-H]^-$	m/z	Δppm	RDB	Charge, z
$C_6H_{11}O_7^-$ (C_6)	195.04880	-0.789	1.5	1
$C_5H_{10}O_5$ (r-C_5)	149.04344	-1.776	1.5	1
$C_3H_5O_4^-$ (C_3)	105.01750	-2.000	1.5	1
$C_3H_6O_3$ (r-C_3)	89.02254	-3.768	1.5	1
$C_2H_4O_2$ (r-C_2)	59.01218	-4.759	1.5	1

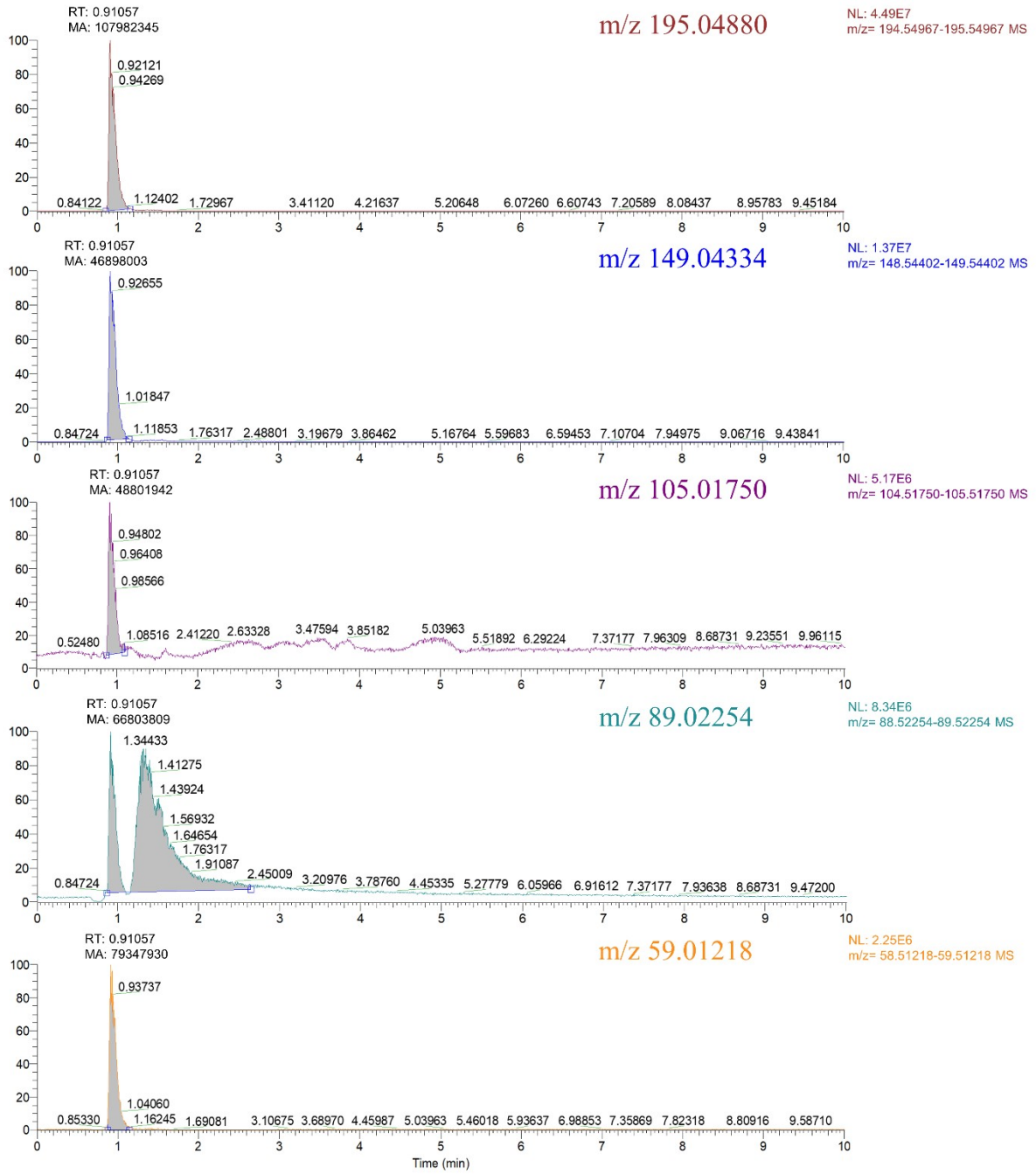

Fig. S17 Chromatograms for extracted-ions from LC-MS analysis in the solution of xylose photoreforming containing Ag-SNGODs.

Chemical Formula	Retention time RT (min)	Base peak (m/z)	Measured Area MA
$C_6H_{11}O_7^-$ (C_6)	0.91057	195.04880	125755825
$C_5H_{10}O_5$ (r-C_5)	0.91057	149.04344	60362796
$C_3H_5O_4^-$ (C_3)	0.91057	105.01750	62813371
$C_3H_6O_3$ (r-C_3)	0.91057	89.02254	85983719
$C_2H_4O_2$ (r-C_2)	0.91057	59.01218	97415490

16. LC-MS-MS analysis of the deprotonated products

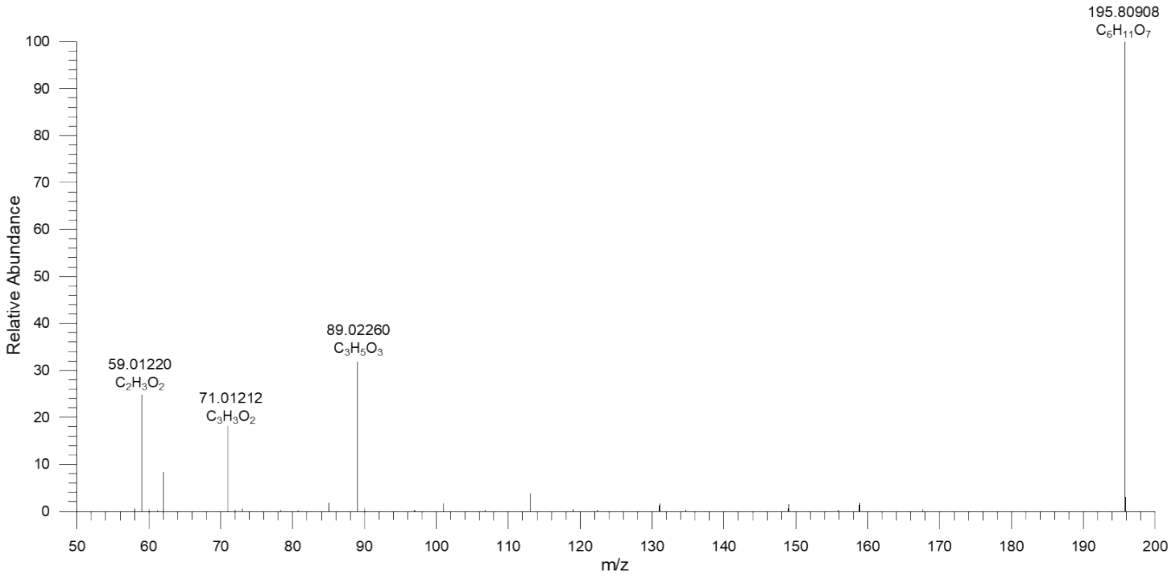

Fig. S18 LC-MS-MS spectrum of the deprotonated $C_6H_{11}O_7$ compound (m/z 195). These fragments of the deprotonated $C_6H_{11}O_7$ compound (m/z 195) are in agreement with those of gluconate ($C_6H_{11}O_7^-$).

Fragment	m/z	Δppm	RDB
$C_6H_{11}O_7^-$	195.80908	-0.149	1.5
$C_3H_5O_3^-$	89.02260	-3.094	1.5
$C_3H_3O_2^-$	71.01212	-3.955	2.5
$C_2H_3O_2^-$	59.01220	-4.420	1.5

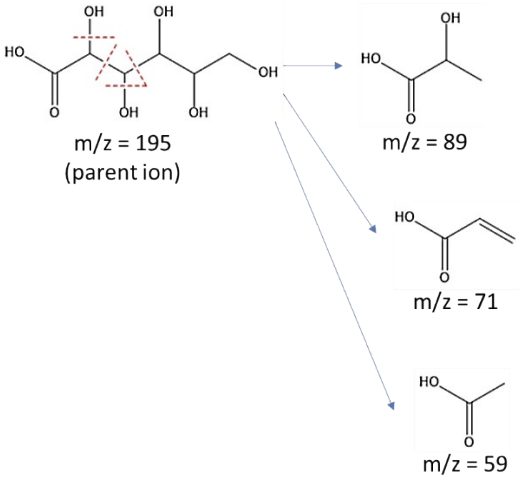

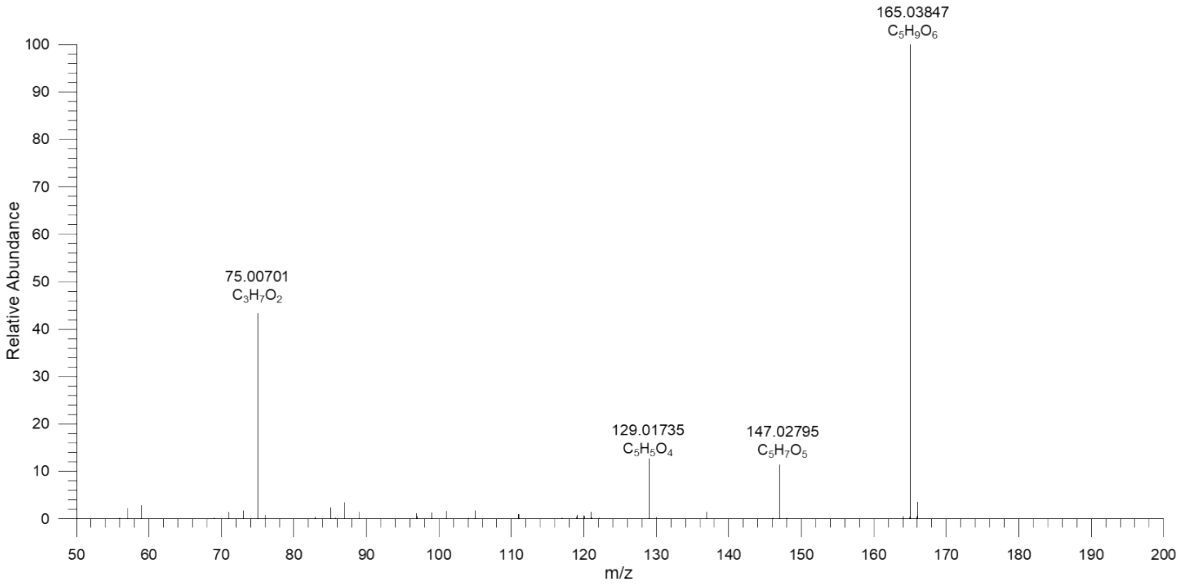

Fig. S19 LC-MS-MS spectrum of the deprotonated $C_5H_9O_6$ compound (m/z 165). These fragments of the deprotonated $C_5H_9O_6$ compound (m/z 165) are in agreement with those of xylonate ($C_5H_9O_6^-$).

Fragment	m/z	Δppm	RDB
$C_5H_9O_6^-$	165.03847	-1.420	1.5
$C_5H_7O_5^-$	147.02795	-5.780	2.5
$C_5H_5O_4^-$	129.01735	-1.861	3.5
$C_3H_7O_2^-$	75.00701	-3.806	1.5

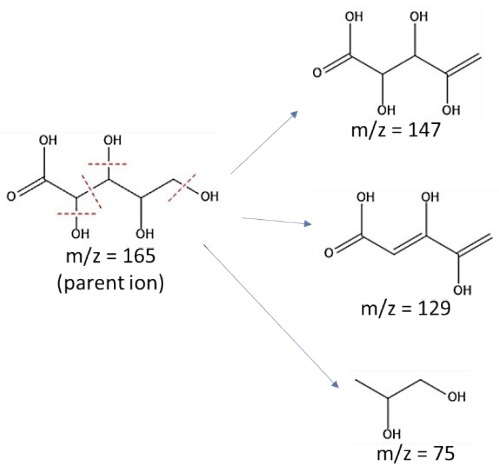

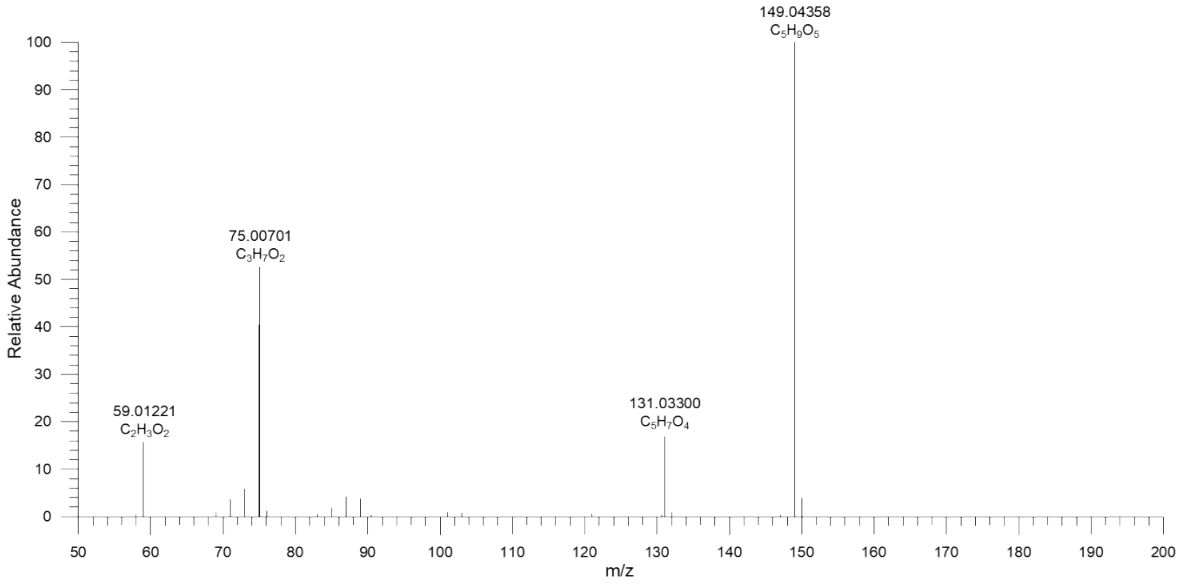

Fig. S20 LC-MS-MS spectrum of the deprotonated $C_5H_9O_5$ compound (m/z 149). These fragments of the deprotonated $C_5H_9O_5$ compound (m/z 149) are in agreement with those of xylose ($C_5H_{10}O_5$).

Fragment	m/z	Δppm	RDB
$C_5H_9O_5^-$	149.04358	-0.836	1.5
$C_5H_7O_4^-$	131.03300	-1.756	2.5
$C_3H_7O_2^-$	75.00701	-3.306	1.5
$C_2H_3O_2^-$	59.01221	-4.250	1.5

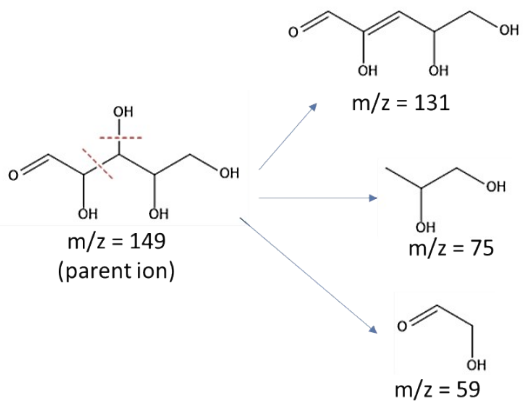

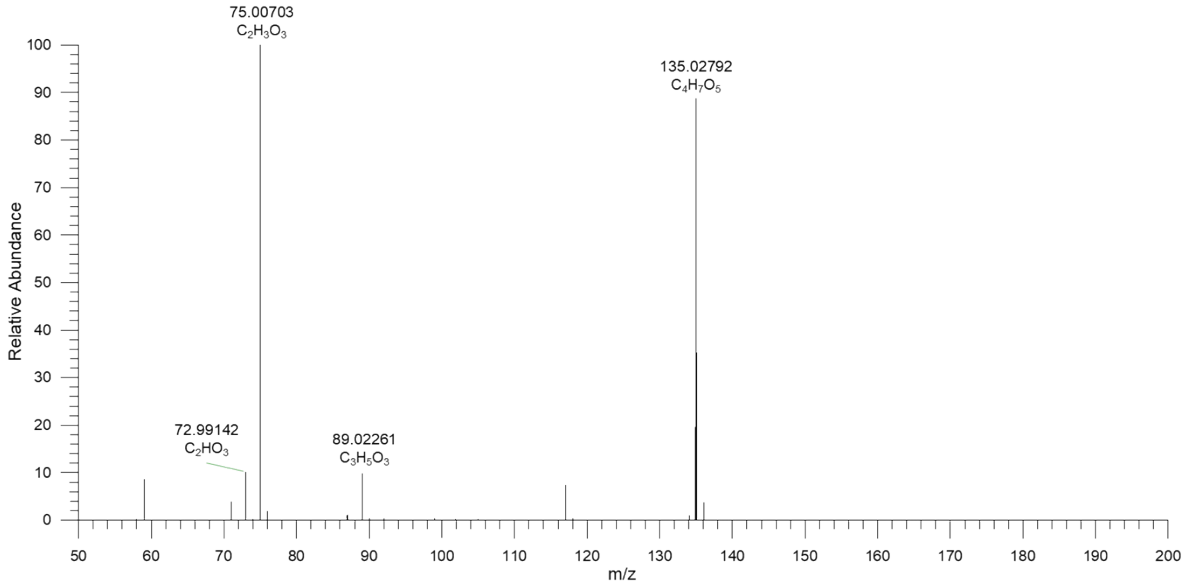

Fig. S21 LC-MS-MS spectrum of the deprotonated $C_4H_7O_5$ compound (m/z 135). These fragments of the deprotonated $C_4H_7O_5$ compound (m/z 135) are in agreement with those of 2,3,4-trihydroxybutanoate ($C_4H_7O_5^-$).

Fragment	m/z	Δppm	RDB
$C_4H_7O_5^-$	135.02792	-1.516	1.5
$C_3H_5O_3^-$	89.02261	-2.982	1.5
$C_2H_3O_3^-$	75.00703	-3.539	1.5
$C_2HO_3^-$	72.99142	-3.226	2.5

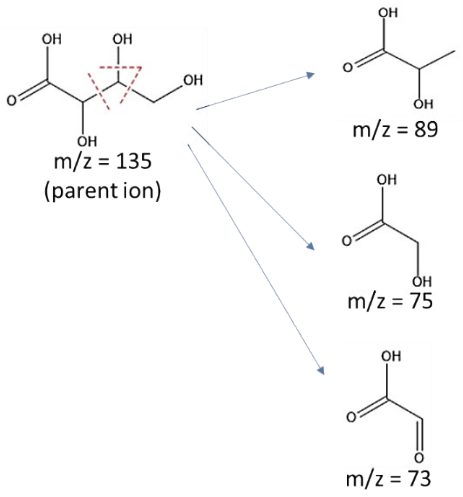

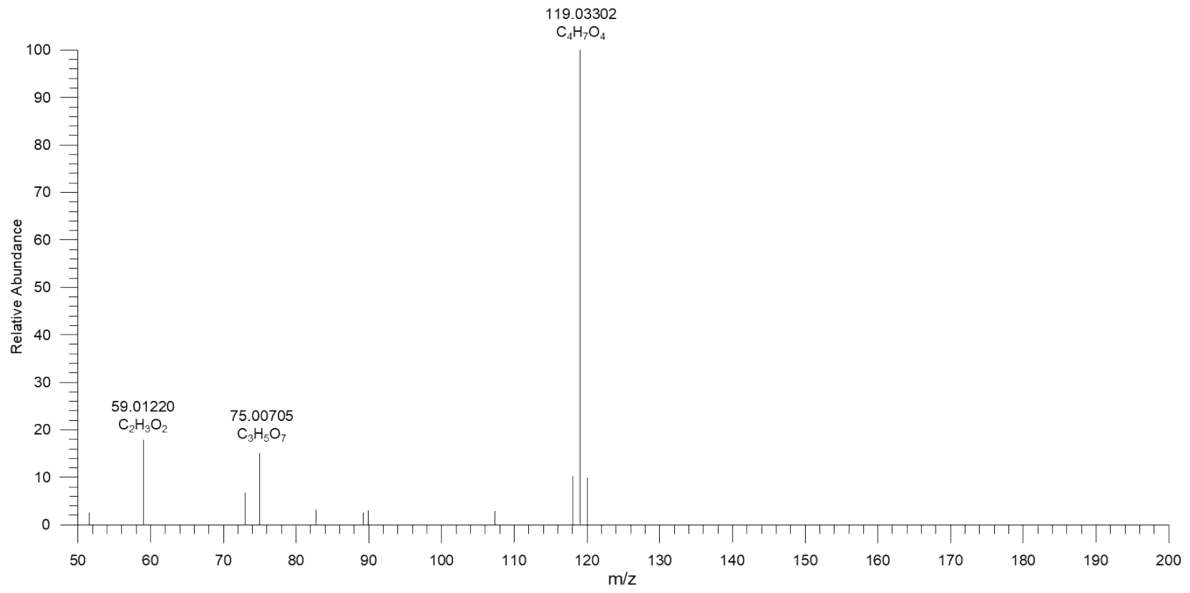

Fig. S22 LC-MS-MS spectrum of the deprotonated $C_4H_7O_4$ compound (m/z 119). These fragments of the deprotonated $C_4H_7O_4$ compound (m/z 119) are in agreement with those of erythrose ($C_4H_8O_4$).

Fragment	m/z	Δppm	RDB
$C_4H_7O_4^-$	119.03302	-2.269	1.5
$C_3H_5O_7^-$	75.00705	-3.272	0.5
$C_2H_3O_2^-$	59.01220	-4.420	1.5

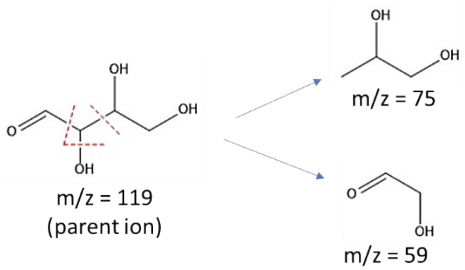

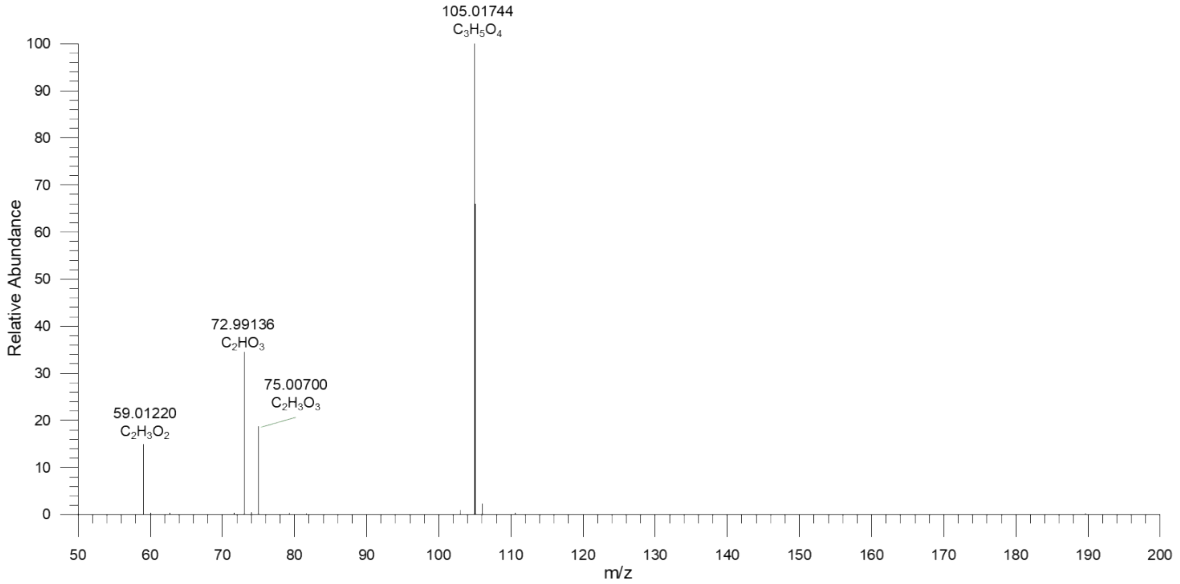

Fig. S23 LC-MS-MS spectrum of the deprotonated $C_3H_5O_4$ compound (m/z 105). These fragments of deprotonated $C_3H_5O_4$ compound (m/z 105) are in agreement with those of glycerate ($C_3H_5O_4^-$).

Fragment	m/z	Δppm	RDB
$C_3H_5O_4^-$	105.01744	-2.572	1.5
$C_2H_3O_3^-$	75.00700	-3.939	1.5
$C_2HO_3^-$	72.99136	-4.048	2.5
$C_2H_3O_2^-$	59.01220	-4.420	1.5

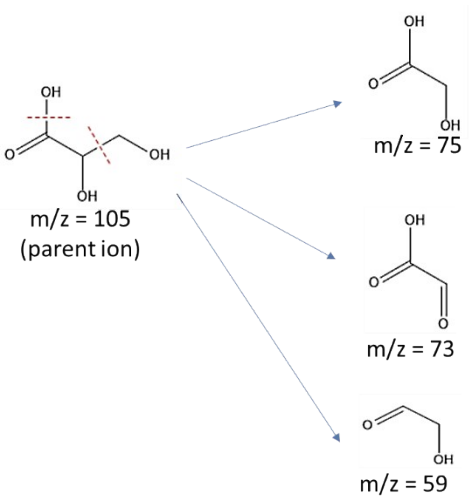

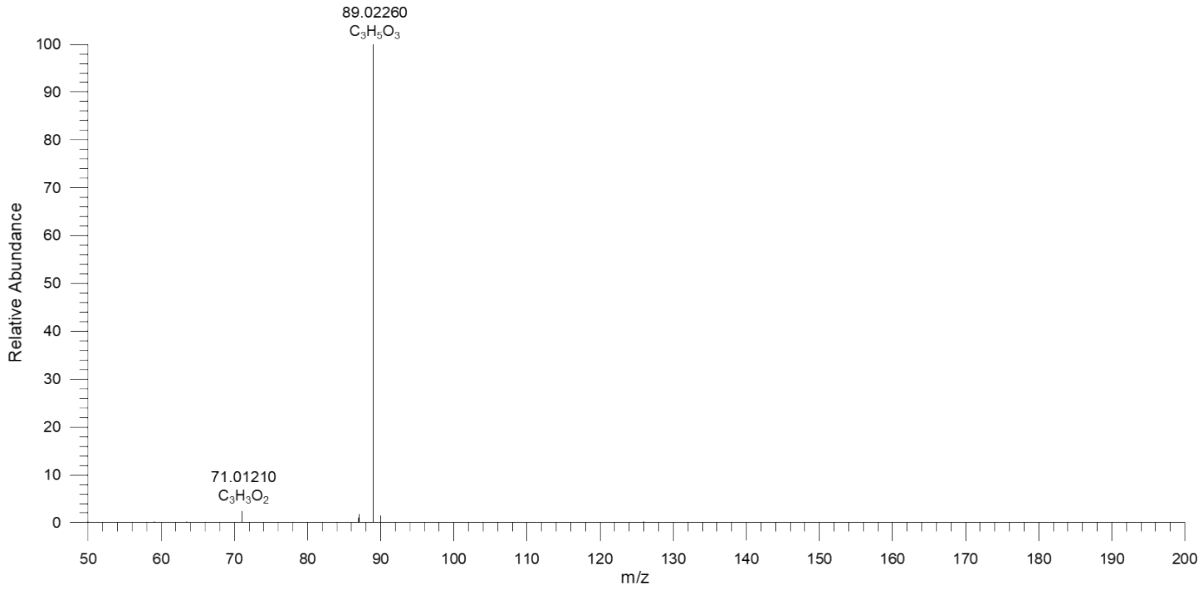

Fig. S24 LC-MS-MS spectrum of the deprotonated $C_3H_5O_3$ compound (m/z 89). These fragments of the deprotonated $C_3H_5O_3$ compound (m/z 89) are in agreement with those of glyceraldehyde ($C_3H_6O_3$).

Fragment	m/z	Δppm	RDB
$C_3H_5O_3^-$	89.02260	-3.094	1.5
$C_3H_3O_2^-$	71.01210	-4.924	2.5

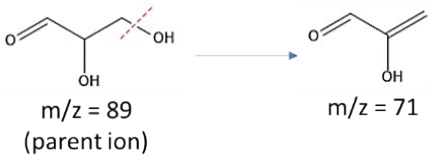

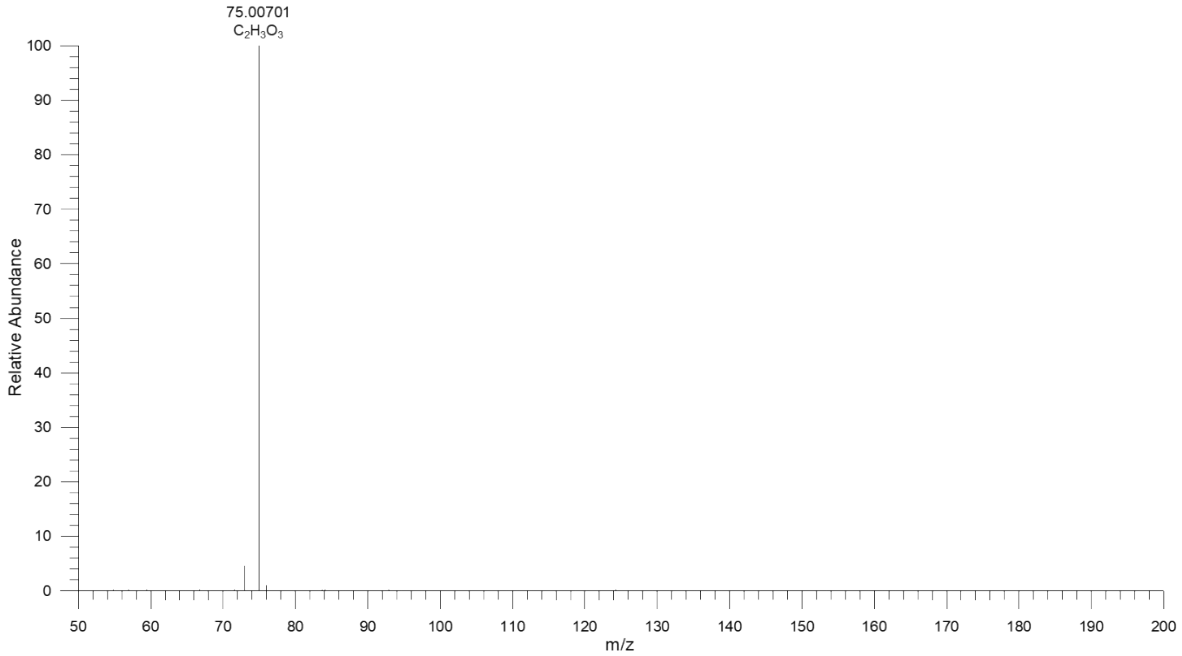

Fig. S25 LC-MS-MS spectrum of the deprotonated $C_2H_3O_3$ compound (m/z 75). These fragments of the deprotonated $C_2H_3O_3$ compound (m/z 75) are in agreement with those of glycolate ($C_2H_3O_3^-$).

Fragment	m/z	Δppm	RDB
$C_2H_3O_3^-$	75.00701	-3.806	1.5

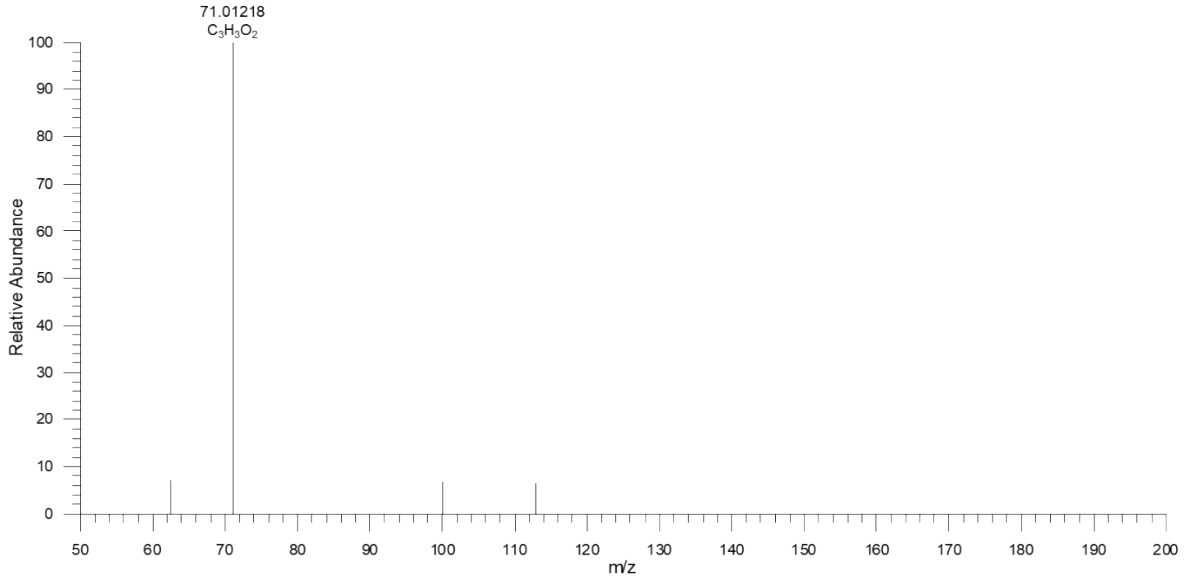

Fig. S26 LC-MS-MS spectrum of the deprotonated $C_3H_3O_2$ compound (m/z 71). These fragments of the deprotonated $C_3H_3O_2$ compound (m/z 71) are in agreement with those of 3-hydroxy-2-propenal ($C_3H_3O_2^-$).

Fragment	m/z	Δppm	RDB
$C_3H_3O_2^-$	71.01218	-3.251	2.5

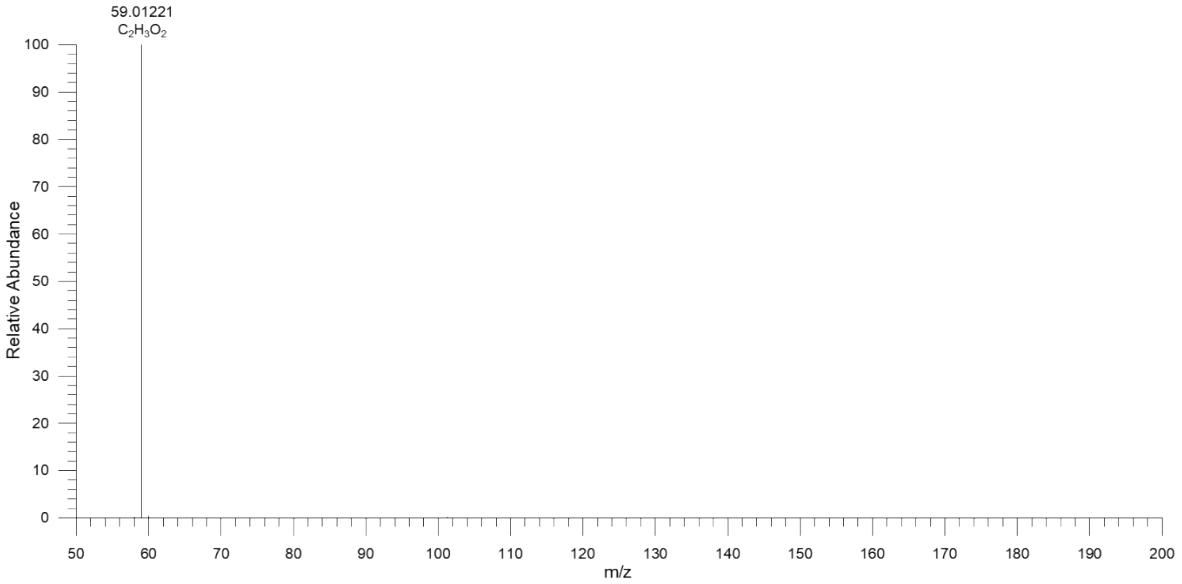

Fig. S27 LC-MS-MS spectrum of the deprotonated $C_2H_3O_2$ compound (m/z 59). These fragments of the deprotonated $C_2H_3O_2$ compound (m/z 59) are in agreement with those of glycolaldehyde ($C_2H_4O_2$).

Fragment	m/z	Δppm	RDB
$C_2H_3O_2^-$	59.01221	-4.250	1.5

17. GC-MS analysis of the solutions from xylose reforming of Pt-SNGODs

Retention time (min)	Name	Area peak
12.883	Acetate	79097
13.425	Propanoate	9903
13.750	Formate	269791
13.925	1,2-Ethanediol	38580

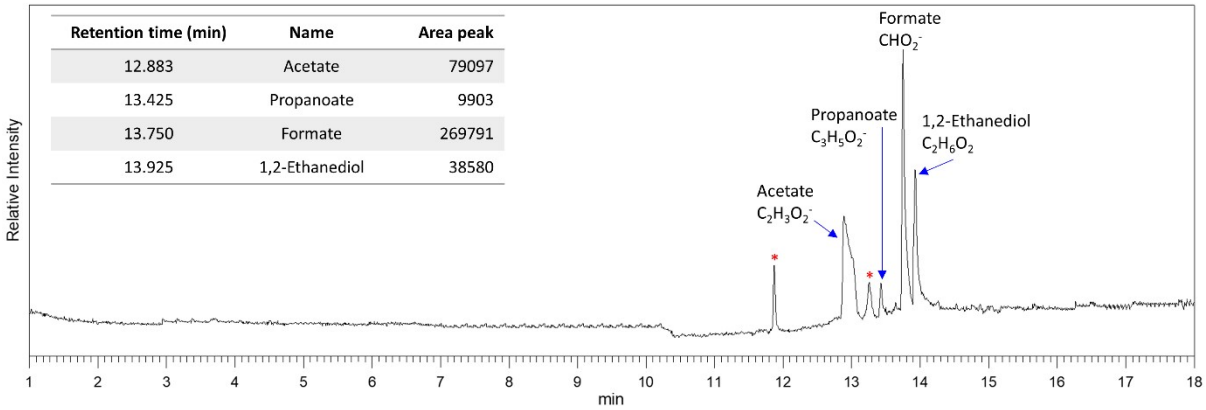

Fig. S28 Liquid products from the GC-MS analysis in the solution of xylose photoreforming containing Pt-SNGODs after 72 h irradiation**.** (*) unknown impurities that are irrelevant to this study.

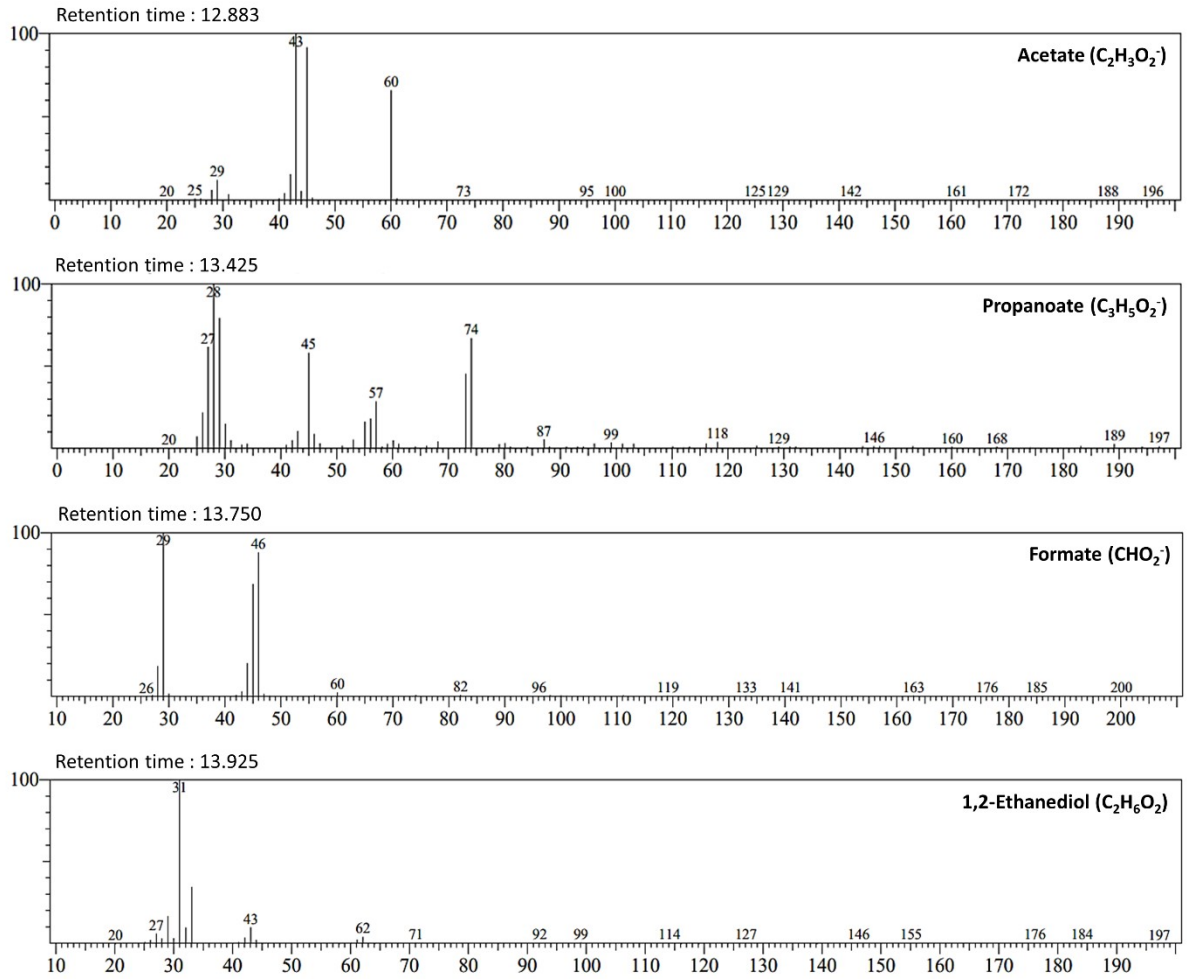

Fig. S29 Mass spectra of the compounds obtained from GC spectra with Pt-SNGODs. All the compounds have been confirmed with the standard solutions.

18. GC-MS analysis of the solutions from xylose reforming of Ag-SNGODs

Retention time (min)	Name	Area peak
12.933	Acetate	228019
13.458	Propanoate	44387
13.758	Formate	90753
13.967	1,2-Ethanediol	149510

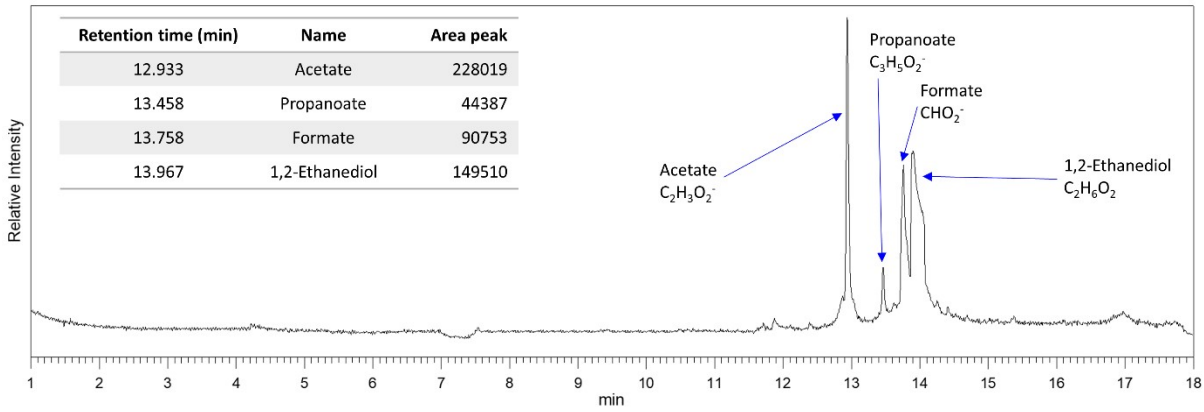

Fig. S30 Liquid products from the GC-MS analysis in the solution of xylose photoreforming containing Ag-SNGODs after 72 h irradiation.

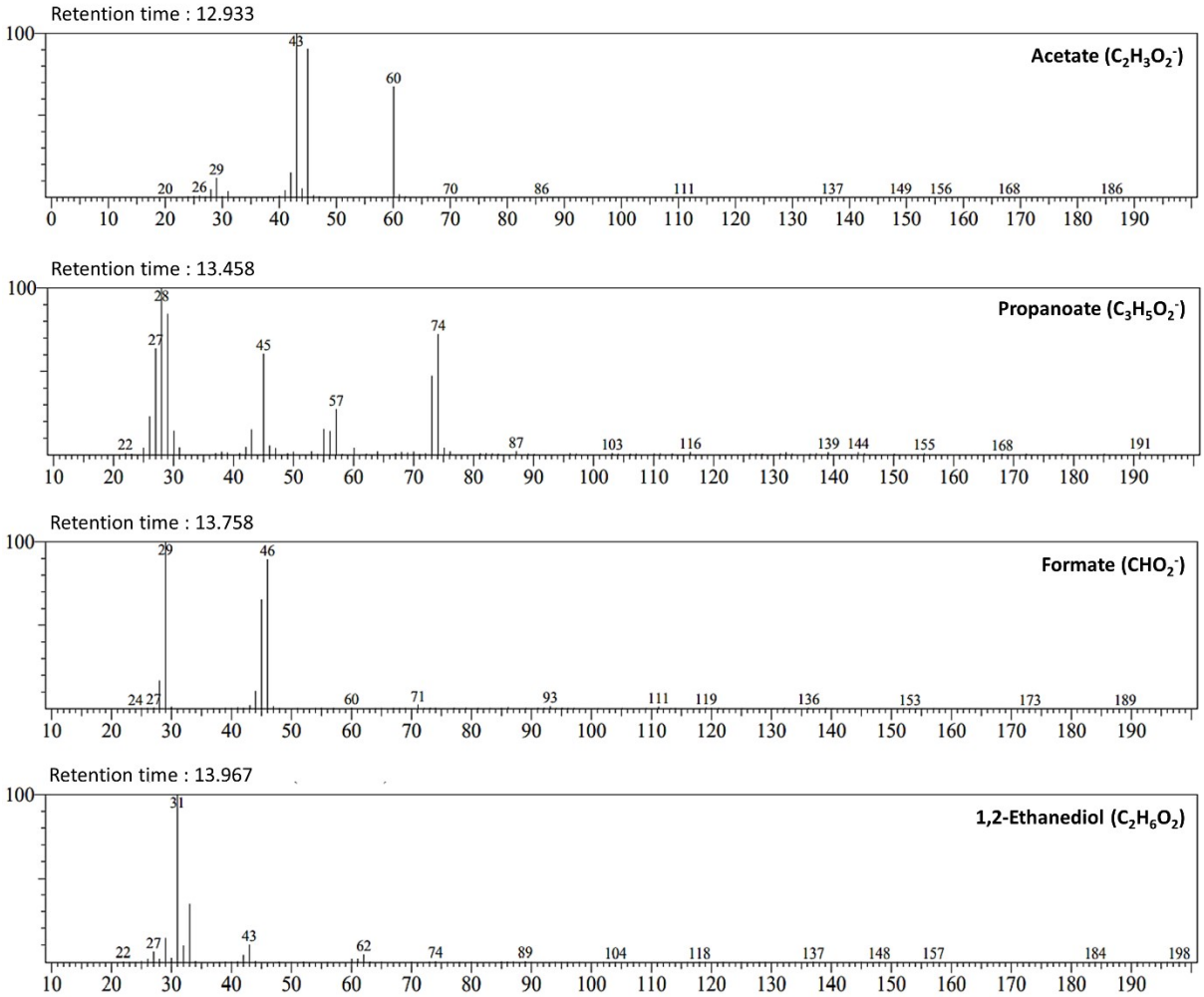

Fig. S31 Mass spectra of the compounds obtained from GC spectra with Ag-SNGODs. All the compounds have been confirmed with the standard solutions.

19. H_2 production from glycolaldehyde and glyceraldehyde

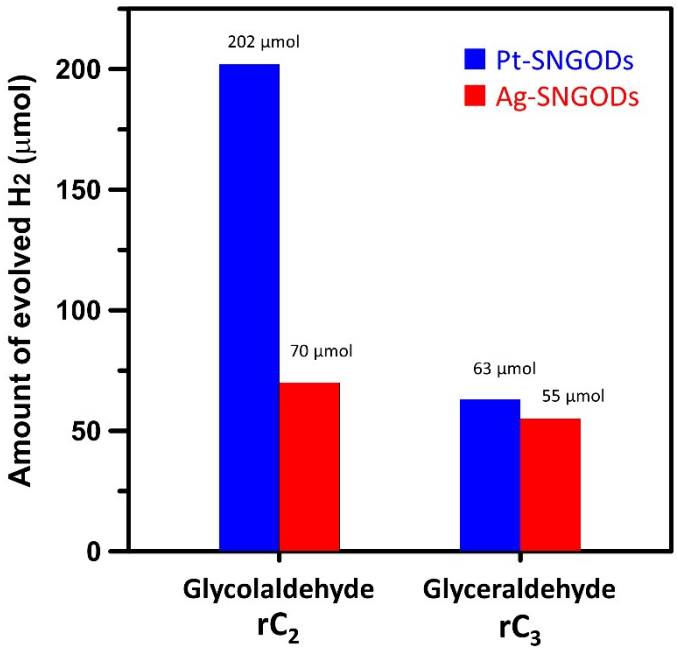

Fig. S32 Photocatalytic reforming of glycolaldehyde and glyceraldehyde over Pt-SNGODs and Ag-SNGODs for H_2 production. The H_2 amounts were obtained after 12 h of reaction.

References

1. Q. Gu, J. Long, L. Fan, L. Chen, L. Zhao, H. Lin and X. Wang, *J. Catal.*, 2013, **303**, 141-155.

2. H. Zhao, C.-F. Li, X. Yong, P. Kumar, B. Palma, Z.-Y. Hu, G. Van Tendeloo, S. Siahrostami, S. Larter and D. Zheng, *Iscience*, 2021, **24**.

3. X. Xu, J. Zhang, S. Wang, Z. Yao, H. Wu, L. Shi, Y. Yin, S. Wang and H. Sun, *J. Colloid Interface Sci.*, 2019, **555**, 22-30.

4. Q. Liu, L. Wei, Q. Xi, Y. Lei and F. Wang, *Chem. Eng. J.*, 2020, **383**, 123792.

5. H. Zhao, P. Liu, X. Wu, A. Wang, D. Zheng, S. Wang, Z. Chen, S. Larter, Y. Li and B.-L. Su, *Appl. Catal. B: Environ.*, 2021, **291**, 120055.

6. G. Iervolino, V. Vaiano, D. Sannino, L. Rizzo and V. Palma, *Appl. Catal. B: Environ.*, 2017, **207**, 182-194.

7. G. Iervolino, V. Vaiano, J. Murcia, L. Rizzo, G. Ventre, G. Pepe, P. Campiglia, M. Hidalgo, J. A. Navío and D. Sannino, *J. Catal.*, 2016, **339**, 47-56.

8. A. Speltini, A. Scalabrini, F. Maraschi, M. Sturini, A. Pisanu, L. Malavasi and A. Profumo, *Int. J. Hydrogen Energy*, 2018, **43**, 14925-14933.

9. Q. Liu, F. Wang, Y. Jiang, W. Chen, R. Zou, J. Ma, L. Zhong and X. Peng, *Carbon*, 2020, **170**, 199-212.